ARMY RESEARCH LABORATORY

Poly(aryl-ether-ether-ketone) as a Possible Metalized Film Capacitor Dielectric: Accurate Description of the Band Gap Through Ab Initio Calculation

by Janet Ho, Marco Olguin, and Carlos Diaz

ARL-TR-7160 **December 2014**

NOTICES

Disclaimers

The findings in this report are not to be construed as an official Department of the Army position unless so designated by other authorized documents.

Citation of manufacturer's or trade names does not constitute an official endorsement or approval of the use thereof.

Destroy this report when it is no longer needed. Do not return it to the originator.

Army Research Laboratory
Adelphi, MD 20783-1138

ARL-TR-7160 **December 2014**

Poly(aryl-ether-ether-ketone) as a Possible Metalized Film Capacitor Dielectric: Accurate Description of the Band Gap Through Ab Initio Calculation

Janet Ho and Marco Olguin
Sensors and Electron Devices Directorate, ARL

and

Carlos Diaz
ARL Summer Student, University of Texas at El Paso, TX

REPORT DOCUMENTATION PAGE	Form Approved OMB No. 0704-0188

1. REPORT DATE *(DD-MM-YYYY)*	2. REPORT TYPE	3. DATES COVERED (From - To)
December 2014	Final	

4. TITLE AND SUBTITLE	5a. CONTRACT NUMBER
Poly(aryl-ether-ether-ketone) as a Possible Metalized Film Capacitor Dielectric: Accurate Description of the Band Gap Through Ab Initio Calculation	5b. GRANT NUMBER
	5c. PROGRAM ELEMENT NUMBER

6. AUTHOR(S)	5d. PROJECT NUMBER
Janet Ho, Marco Olguin, and Carlos Diaz	5e. TASK NUMBER
	5f. WORK UNIT NUMBER

7. PERFORMING ORGANIZATION NAME(S) AND ADDRESS(ES)	8. PERFORMING ORGANIZATION REPORT NUMBER
US Army Research Laboratory ATTN: RDRL-SED-C 2800 Powder Mill Road Adelphi, MD 20783-1138	ARL-TR-7160

9. SPONSORING/MONITORING AGENCY NAME(S) AND ADDRESS(ES)	10. SPONSOR/MONITOR'S ACRONYM(S)
	11. SPONSOR/MONITOR'S REPORT NUMBER(S)

12. DISTRIBUTION/AVAILABILITY STATEMENT

Approved for public release; distribution unlimited.

13. SUPPLEMENTARY NOTES

14. ABSTRACT

Poly(aryl-ether-ether-ketone) (PEEK) is a primary candidate for a high temperature capacitor dielectric due to its outstanding mechanical strength and thermal stability. However, its breakdown strength is unsatisfactory (~400 MV/m) and its volumetric resistivity drops significantly at electric fields above 100 MV/m. Our main objective is to study the effect of chemical impurities, such as water molecules and chain ends, on impurity states in the band gap of PEEK using density functional theory (DFT) to gain insight on the factors impacting electrical resistivity under a high field, which may correlate to low breakdown strength. Our focus is to determine the correct geometry of the unit cell and develop a methodology for computing the band gap of PEEK accurately. We used dispersion-corrected DFT to optimize various starting geometries and determined the correct one based on a comparison with experimental crystallographic data. The band gap was determined from the projected density of states, which is calculated using the HSE06 hybrid exchange-correlation functional. The original HSE06 formulation overestimates the band gap of PEEK by 33% compared to the experimental value. So, to obtain a more accurate functional form, we conducted a systematic study on the parameter space of the functional by varying the exchange-correlation mixing and screening coefficients.

15. SUBJECT TERMS

PEEK, high temperature dielectrics, electronic structure, breakdown strength

16. SECURITY CLASSIFICATION OF:			17. LIMITATION OF ABSTRACT	18. NUMBER OF PAGES	19a. NAME OF RESPONSIBLE PERSON
A. Report	b. ABSTRACT	c. THIS PAGE			Janet Ho
Unclassified	Unclassified	Unclassified	UU	22	19b. TELEPHONE NUMBER (*Include area code*) (301) 394-0051

Standard Form 298 (Rev. 8/98)
Prescribed by ANSI Std. Z39.18

Contents

Lists of Figures

List of Tables

Acknowledgments

We greatly appreciated Professor Rampi Ramprasad from University of Connecticut for the valuable discussion.

INTENTIONALLY LEFT BLANK.

1. Introduction

The demand for high temperature capacitor dielectrics in power electronics is increasing with electrification of military propulsion and weapons systems. Moving toward wide bandgap semiconductors (e.g., silicon carbide [SiC]) will enable operating temperatures above 140 °C, which eases thermal management. However, such systems cannot be designed efficiently unless capacitors are available that can operate at similarly high temperatures. Metalized polymer film capacitors have the advantage of self-healing, which allows graceful failure, i.e., a gradual loss in capacitance, rather than catastrophic failure as in ceramic or film/foil counterparts. As a result, the capacitor dielectric can be operated at an electric field near dielectric breakdown, thus achieving a higher energy density. Presently, the widely used dielectrics are biaxially oriented polypropylene (PP) and poly(ethylene terephthalate) (PET), which are low cost, available in thin film (>0.5 μm in the case of PET and >2.5 μm for PP), and have a relatively high breakdown field (E_{bd} > 550 MV/m). Another important attribute that PP offers is a low dissipation factor (tan δ ~1x 10^{-4}) that is independent of frequency. In comparison, PET is rather lossy (tan δ ~1x10^{-2}), even though its dielectric constant is about 3.2, which is 50% higher than PP. The major disadvantage of both of these dielectrics is that the maximum operating temperature is 100 °C for PP and 125 °C for PET. Based on these materials, the capacitors occupy about 25% of volume in the entire system. Therefore, alternative dielectrics that can operate at high temperatures are needed to alleviate thermal management and improve the overall energy density (volume efficiency).

Some of the high temperature polymers that are available in commercial thin films (10 μm or less) include poly(phenylene sulfide) (PPS), poly(ether-ether-ketone) (PEEK), and poly(ether imide) (PEI), the chemical structures and thermal properties of which are shown in Fig. 1. PP and PET are also included for comparison.

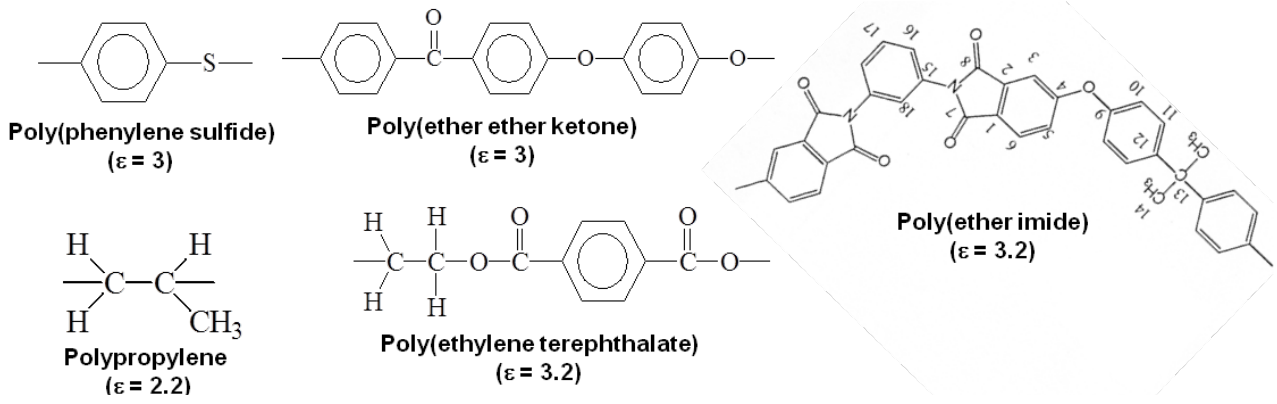

Fig. 1 Chemical structures of the repeating units of various heat-resistant polymers

Among the three high temperature polymers, PEEK has potential due to its strong mechanical/thermal stability, as indicated by its relatively high T_g and T_m, as shown in Table 1. Based on previous results from electrical/dielectric characterization, PEEK has other positive attributes. One of them is a relatively low dissipation at 10 kHz (the typical operating frequency for power conditioning type applications) for temperatures above 110 °C. A comparison of the loss tangent of the polymers is shown in Fig. 2. Another positive attribute that PEEK has is the rather high volumetric resistivity at elevated temperatures for fields below 100 MV/m, as shown in Fig. 3. However, the volumetric resistivity decreases significantly as the field is increased further. Another limitation of PEEK is the relatively low breakdown field (~400 MV/m) compared to the other polymers, as indicated in Fig. 4.

Table 1 Thermal properties of various heat resistant polymers

Polymer	**T_g [a] (°C)**	**T_m [b] (°C)**	**Percent Crystallinity**	**Dielectric Constant**
PPS	120	285	~40	~3
PEEK	150	340	~30	3.1
PEI	220	none	none	3.2
PET	75-80	255	~50	~3.2
PP	<25	170	>60	2.25

[a] T_g denotes glass transition temperature.
[b] T_m denotes crystal melting temperature.

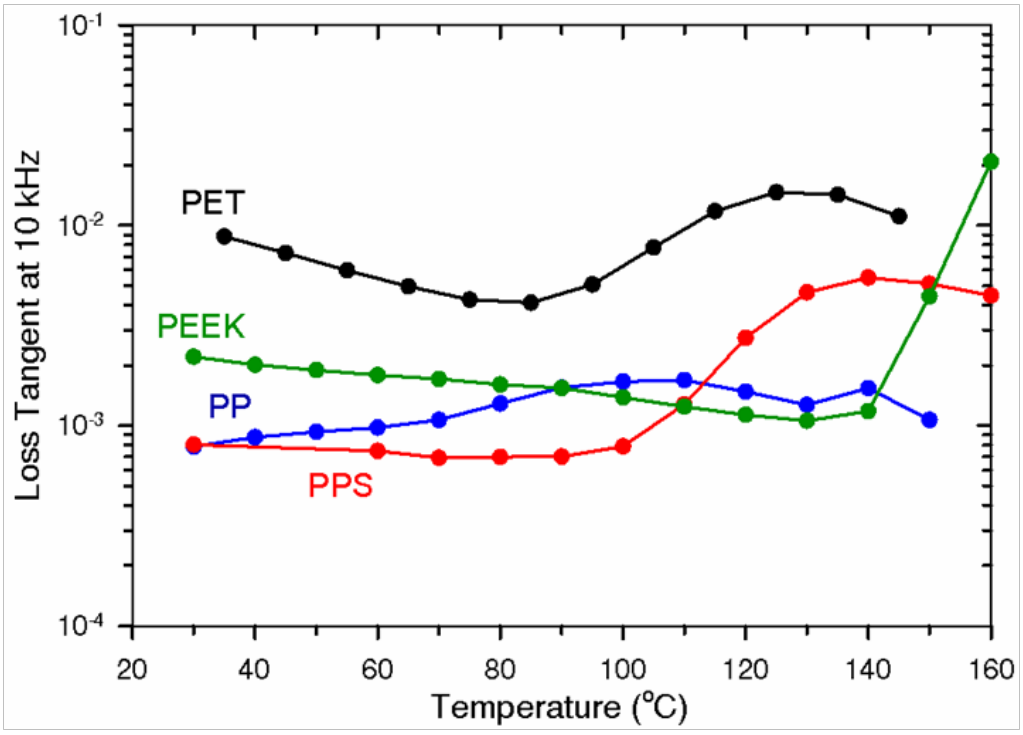

Fig. 2 Loss tangent at 10 kHz as a function of temperature for various polymers

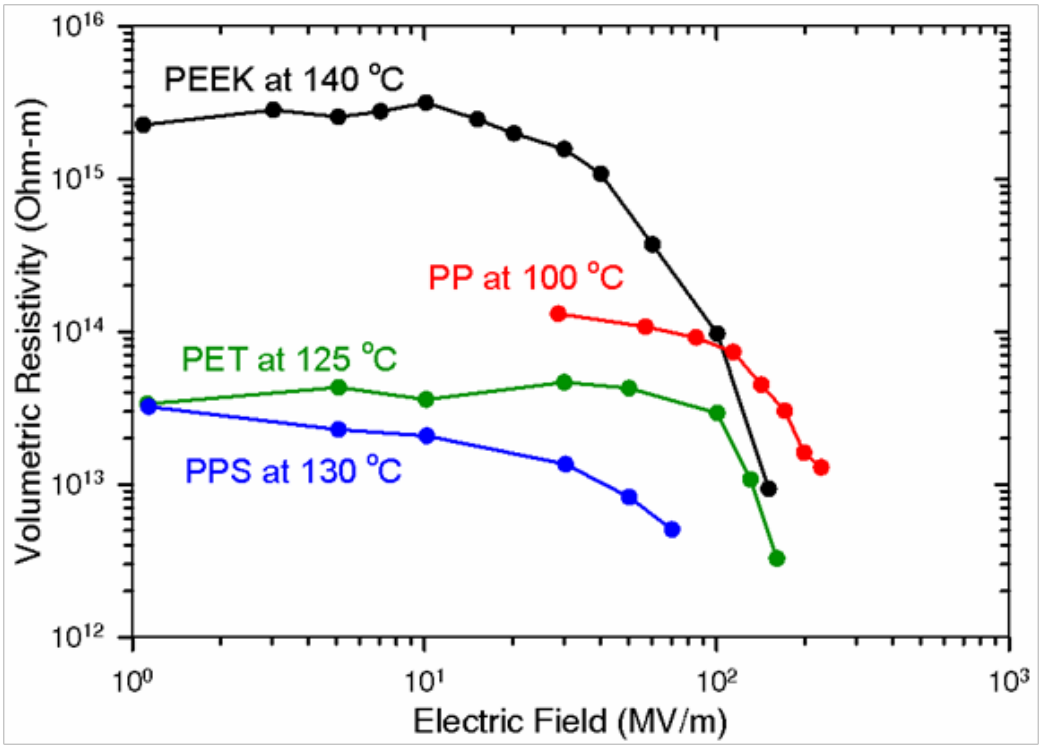

Fig. 3 Volumetric resistivity as a function of electric field at elevated temperature for various polymers

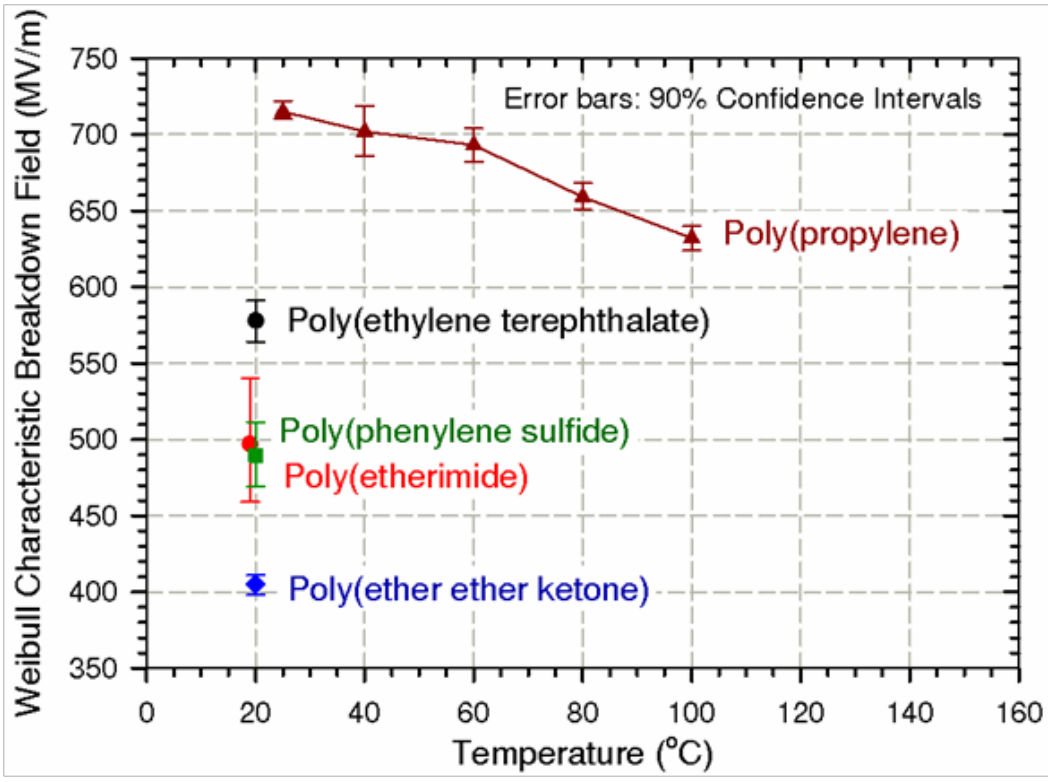

Fig. 4 Weibull characteristic breakdown field for various polymers

In order to gain a fundamental understanding of the underlying causes and mechanisms that lead to high field conduction and low breakdown field, we aim to study the electronic structure of PEEK and investigate the effects of chemical impurities, such as water molecules, and defects, such as chain ends, on the band gap through ab initio calculations. In particular, our goal is to determine if any intermediate energy states (impurity states) are introduced in the band gap. In this report, progress on the study of electronic structure and band-gap calculation of pristine PEEK is summarized.

2. Computational Methodology

All quantum mechanical calculations were performed using density functional theory (DFT) methods with a mixed Gaussian and plane-wave (GPW)[1,2] approach as implemented in the CP2K[3] package. The exchange-correlation functional was described by the generalized gradient approximation (GGA) with the spin-polarized functional developed by Perdew-Burke-Ernzerhof (PBE).[4] Grimme's D3 pair-wise dispersion correction (DFTD3)[5] was employed to account for van der Waals interaction. Wavefunctions were expanded in valence triple-zeta plus polarization (TZVP) Gaussian basis sets[6] with an auxiliary plane-wave basis with a cutoff energy of 900 Rydberg (Ry). The plane-wave cutoff of 900 Ry was determined by converging the energy with respect to the plane-wave cutoff to 1 meV per atom. Core electrons were modeled by the Goedecker-Teter-Hutter (GTH)[7] scalar relativistic norm-conserving pseudopotentials with 1, 4, and 6 valence electrons for hydrogen (H), carbon (C), and oxygen (O), respectively. Brillouin zone integration was performed with a reciprocal space mesh consisting of only the Γ-point.

The initial geometry for all calculations was constructed based on the crystal unit cell parameters of the 6-ring (i.e., 2 repeating units of PEEK) model developed by Iannelli.[8] In order to reduce errors due to periodic approximations, the crystal unit cell, which comprised of 2 chains of 2 repeating units, was doubled along the y-axis to create a supercell of 4 chains, totaling 272 atoms. The supercell is repeated using periodic boundary conditions to simulate an infinite system. Each supercell was optimized by allowing the lattice vectors and lattice angles to shift. Initial geometry optimizations were performed at the PBE+DFTD3/TZVP level of theory with a convergence criterion of 0.02 eV/Å or less for the force on each atom.

After geometry optimization, the ground-state (i.e., temperature at 0 K) electronic structure of PEEK was determined, from which the electron density, density of states (DOS), projected density of states (PDOS), and band gap can be determined. Initial calculations using the PBE-GGA exchange-correlation functional failed to determine the band gap accurately; therefore, we performed single-point calculations using the hybrid functional developed by Heyd-Scuseria-Ernzerhof (HSE06)[9] on the optimized structure described previously. This approach was validated on the band gap of polyethylene with 100% agreement.

For large systems (e.g., PEEK) described with high-quality basis sets, calculation of the Hartree-Fock exact-exchange (HFX) component in the exchange-correlation functional, such as that incorporated in the HSE06 functional, is computationally demanding. To speed up the calculations, we employed the auxiliary density matrix method (ADMM),[10] which has been shown to outperform the standard HFX implementation by a factor of 20 with excellent performance and good accuracy. In this work, the ADMM was employed with the TZVP GTH primary basis set and FIT3 auxiliary fit basis set.

To reassure that the computed structure represents the system under investigation, we compared the computed x-ray diffraction (XRD) pattern with our measurement. The XRD calculations reported in this work employ the method implemented by Krack and co-workers[11] in the CP2K code, in which the elastic or coherent x-ray scattering intensities *I(q)* within the first Born approximation for systems where no angular resolution exists are given by

$$I(q) = \langle |F(\mathbf{q})|^2 \rangle, \tag{1}$$

where

$$F(\mathbf{q}) = \int n(\mathbf{r}) e^{i\mathbf{qr}} d\mathbf{r}, \tag{2}$$

is the Fourier transform of the 1-electron density $n(\mathbf{r})$, $\mathbf{r}$ is the position, $\mathbf{q}$ is the scattering vector, and the average in *I(q)* is over all $\mathbf{q}$ vectors with the same modulus q in the statistical ensemble. $F(\mathbf{q})$ was calculated using the all-electron Gaussian augmented plane-wave (GAPW)[1,2] method, in which the Kohn–Sham orbitals are expanded in plane-waves with the electronic charge density divided into a smooth part that is expanded in plane-waves and an atom-centered, more rapidly varying part, which is expanded in Gaussian functions. As pointed out by Krack, the all-electron method was employed instead of the plane-wave-pseudopotential approach since the latter tends to give an incorrect description of the electronic charge density close to the nuclei. The Becke, Lee, Yang, and Parr (BLYP)[12,13] semilocal form of the exchange-correlation functional was used in all XRD calculations. Other functionals such as PBE, B3LYP[14], and HSE06 were also compared, and no significant difference from BLYP was found.

3. Results

Three initial geometries of PEEK were constructed to determine the best representation for our system. As shown in Fig. 5, Geometry I was created by adapting the unit cell report by Iannelli without any manipulation of the chains, while Geometry II was constructed by shifting the second chain in the unit cell by half of the unit cell length relative to first one along the z-axis and Geometry III was generated by rotating the second chain 90° around the z-axis relative to the first one. All three geometries contain two unit cells along the y-axis. Table 2 summarizes the supercell parameters of the three optimized geometries and the deviation denoted by Δ from the

literature values.[8,15] As indicated in Table 2, the optimized Geometry III gives the best agreement with the literature values. The finding is further supported by the computed XRD patterns, which are shown in Fig. 6. These results serve as an assurance that the ground-state (i.e., temperature at 0 K) Geometry III computed by DFT, which agrees well with experimental measurements, may be used for future calculations.

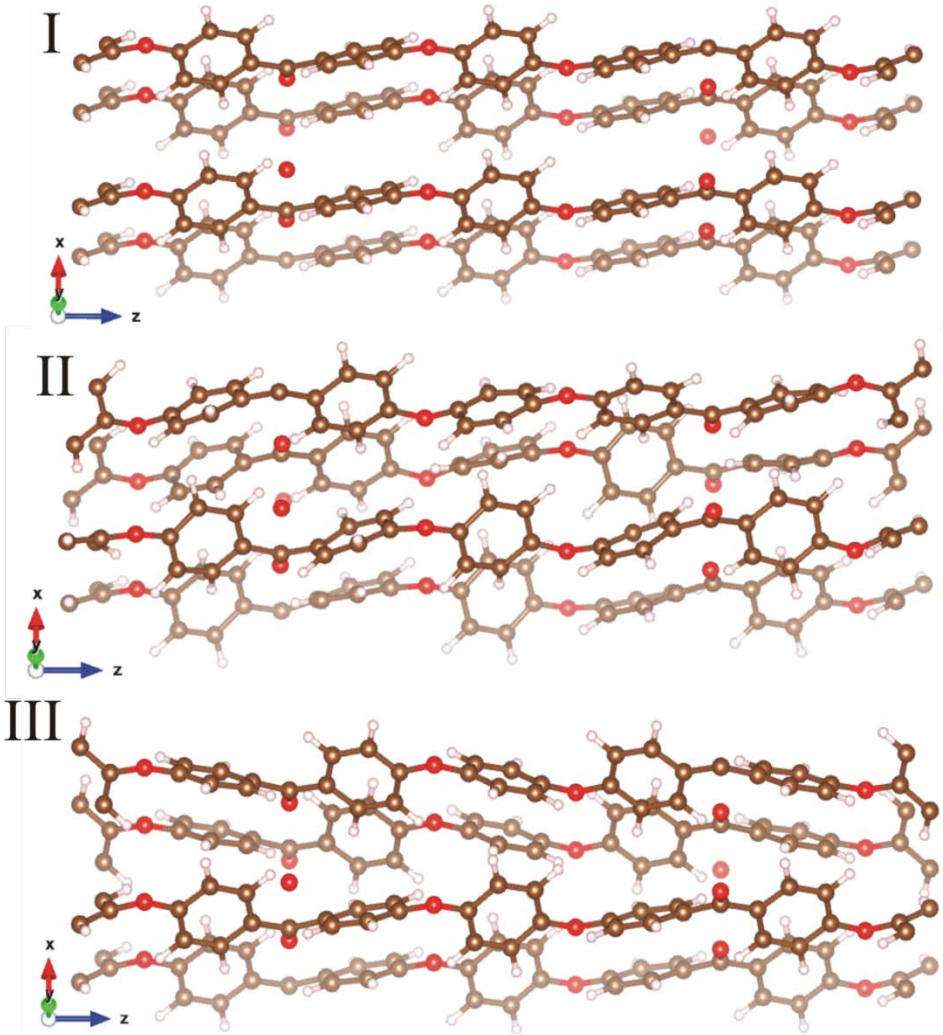

Fig. 5 Illustration of the 3 optimized supercells. Chains in a lighter color represent ones in the background.

Table 2 Comparison of the structure parameters of the 3 optimized supercells with literature

	Literature	**I**	**II**	**III**
a / Δ (Å)	7.78 /--	9.30 / *+1.52*	7.77 / *–0.01*	7.58 / *–0.2*
b / Δ (Å)	11.84 /--	11.74 / *–0.1*	12.46 / *+0.62*	11.89 / *+0.05*
c / Δ (Å)	29.92 /--	30.21 / *+0.29*	29.83 / *–0.09*	30.05 / *+0.13*
α / Δ (deg.)	90.0 /--	91.16 / *+1.16*	89.96 / *–0.04*	89.89 / *–0.11*
β / Δ (deg.)	90.0 /--	118.43 / *+28.43*	89.80 / *–0.2*	90.04 / *+0.04*
γ / Δ (deg.)	90.0 /--	80.19 / *–9.81*	90.10 / *+0.1*	90.02 / *+0.02*
Volume / Δ ($Å^3$)	2756 /--	2851 / *+95*	2888 / *+132*	2708 / *–48*

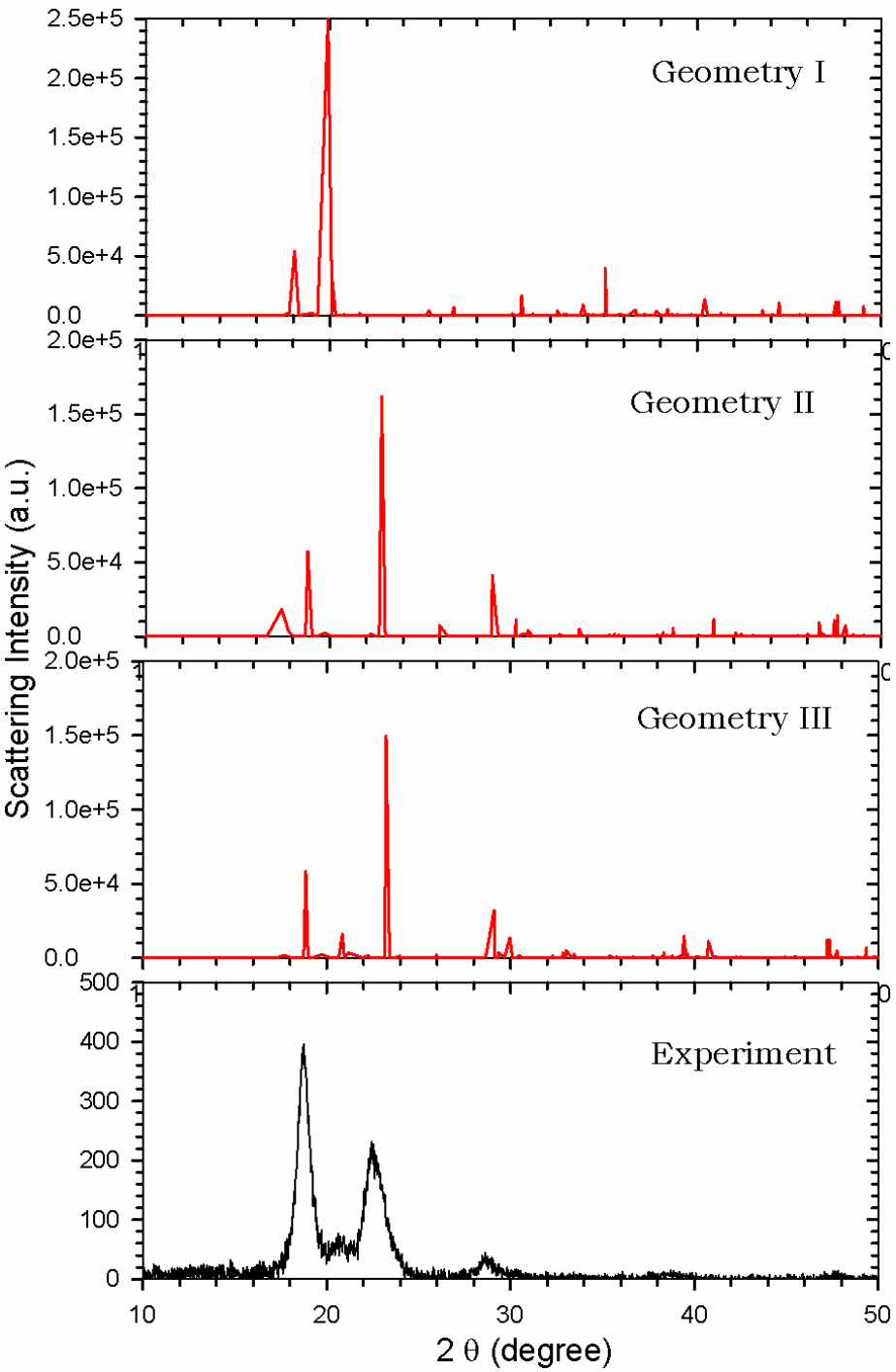

Fig. 6 Comparison of the computed XRD patterns for the 3 optimized geometries with the experiment

Geometry III was used as the basis for calculating the DOS of PEEK, which is shown in Fig. 7a, from which the band gap was determined as 4.21 eV, which is 33% higher than the experimental value of 3.1 eV calculated based on the ultraviolet (UV) cut-off wavelength of 390 nm shown in Fig. 8 by

$$E_g = hc/\lambda, \quad (3)$$

where E_g is the band gap, h the Planck constant in eV-s, c the speed of light in nm/s, and λ the UV cutoff wavelength in nm. The discrepancy is the consequence of the approximation within DFT for describing the exchange-correlation energy of electrons, for which the HSE06 hybrid functional was used in this work. To obtain better agreement for the band gap value for future calculations, a systemic study was conducted for the (α, ω) parameter space of the HSE functional, where α is the exchange mixing coefficient that determines the amount of exact exchange, and ω is the screening parameter controlling short-range interaction. The band gap converged to around experimental value at α = 0.093 and ω = 0.11 bohr^{-1}. The corresponding DOS is shown in Fig. 7b; whereas, the one shown in Fig. 7a was computed from α = 0.25 and ω = 0.11 (these parameters are based on the version of Geometry III that was forced to be orthogonal). Future HSE calculations will be performed with the updated parameters.

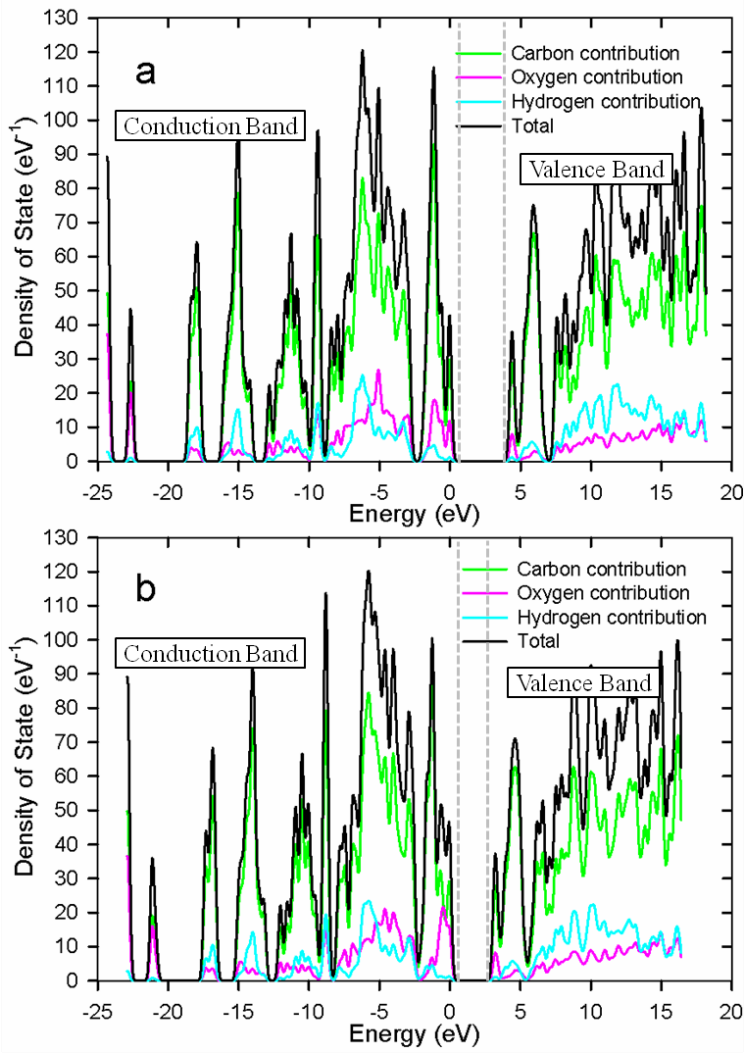

Fig. 7 Density of States of PEEK based on the optimized Geometry III: a) from standard HSE06 hybrid functional with α = 0.25 and ω = 0.11 bohr^{-1} and b) from HSE with α = 0.093 and ω of 0.11 bohr^{-1}

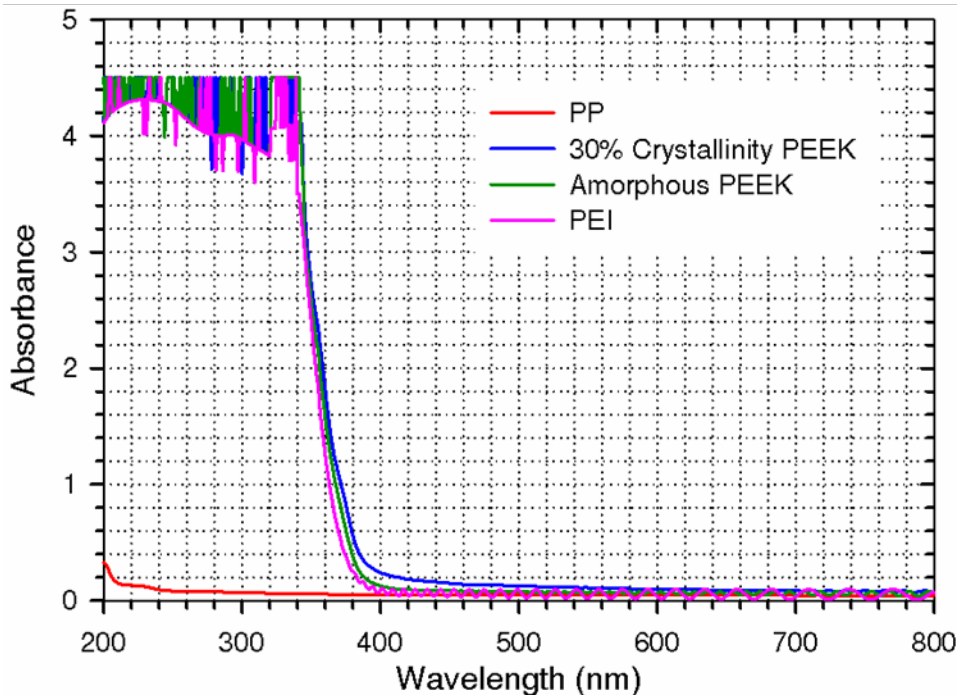

Fig. 8 UV absorption spectra of amorphous and semi-crystalline PEEK. PP and PEI are included for comparison

4. Conclusion

The correct geometry of the unit cell and a methodology for computing accurately the band gap of PEEK were developed. Dispersion-corrected DFT was used to optimize various starting geometries, and the correct one was determined based on a comparison with experimental crystallographic data. The band gap was determined from the PDOS, which is calculated using the HSE06 hybrid exchange-correlation functional. The original formulation of the HSE06 functional overestimates the band gap of PEEK by 33% in comparison to the experimental value. Therefore, a systematic study of the parameter space of the functional was conducted by varying the exchange-correlation mixing and screening coefficients to obtain a functional form that best reproduces the experimental value of the band gap.

5. References

1. Lippert G, Hutter J, Parrinello M. Mol. Phys. 1997;92:477−487.
2. Lippert G, Hutter J, Parrinello M. Theor. Chem. Acc. 1999;103:124.
3. CP2K version 2.5. CP2K is freely available from www.cp2k.org
4. Perdew J, Burke K, Ernzerhof M. Phys. Rev. Lett. 1996;77:3865–3868.
5. Grimme S, Antony J, Ehrlich S, Krieg H. J. Chem. Phys. 2010;132:154104.
6. VandeVondele J, Hutter J. J. Chem. Phys. 2007;127:114105.
7. Goedecker S, Teter M, Hutter J. Phys. Rev. B. 1996;54:1703−1710.
8. Iannelli P. Macromolecules 1993;26:2309–2314.
9. Krukau AV, Vydrov OA, Izmaylov .F, Scuseria GE. J. Chem. Phys. 2006;125:224106.
10. Guidon M, Hutter J, VandeVondele J. J. Chem. Theory Comput. 2010;6(8):2348–2364.
11. Krack M, Gambirasio A, Parrinello M. J. Chem. Phys. 2002;117:9409.
12. Becke AD. Phys. Rev. A. 1988;38:3098.
13. Lee C, Yang W, Parr RG. Phys. Rev. B. 1988;37:785.
14. Stephens PJ, Devlin FJ, Chabalowski CF, Frisch MJ. J. Phys. Chem. 1994;98:11623.
15. Blundell D J, Newton AB. Polymer 1991;32:308.

List of Symbols, Abbreviations, and Acronyms

ADMM	auxiliary density matrix method
BLYP	Becke, Lee, Yang, and Parr
C	carbon
DFT	density functional theory
DFTD3	D3 pair-wise dispersion correction
DOS	density of states
GAPW	Gaussian augmented plane-wave
GGA	generalized gradient approximation
GPW	Gaussian and plane-wave
GTH	Goedecker-Teter-Hutter
H	hydrogen
HFX	Hartree-Fock exact-exchange
HSE	Heyd-Scuseria-Ernzerhof
O	oxygen
PBE	Perdew-Burke-Ernzerhof
PDOS	projected density of states
PEEK	poly(ether-ether-ketone)
PEI	poly(ether imide)
PET	poly(ethylene terephthalate)
PP	polypropylene
PPS	poly(phenylene sulfide)
Ry	Rydberg
SiC	silicon carbide
TZVP	variance triple-zeta plus polarization

UV	ultraviolet
XRD	x-ray diffraction

1 DEFENSE TECH INFO CTR
(PDF) ATTN DTIC OCA

2 US ARMY RSRCH LAB
(PDF) ATTN IMAL HRA MAIL & RECORDS MGMT
ATTN RDRL CIO LL TECHL LIB

1 GOVT PRNTG OFC
(PDF) ATTN A MALHOTRA

4 US ARMY RSRCH LAB
(PDF) ATTN RDRL SED C J HO
ATTN RDRL SED C M OLGUIN
ATTN RDRL SED C R JOW
ATTN RDRL SED P C SCOZZIE

INTENTIONALLY LEFT BLANK.